Valence-band physics and the optical properties of GaN epilayers grown onto sapphire with wurtzite symmetry

Bernard Gil, Olivier Briot, and Roger-Louis Aulombard

Université de Montpellier II, Groupe d'Etude des Semiconducteurs, Case Courrier 074-34095 Montpellier CEDEX 5, France

We report on a quantitative analysis of the band gap of hexagonal GaN epilayers in terms of the joint contributions of the actual wurtzite symmetry on the one hand and of residual strain fields on the other hand. This investigation leads to revision of the previous modelings based on quasicubic descriptions of the valence-band physics and gives $\Delta_1 = 10 \pm 0.1$ meV, $\Delta_2 = 6.2 \pm 0.1$ meV, and $\Delta_3 = 5.5 \pm 0.1$ meV. Last we propose a set of deformation potentials for the hexagonal GaN semiconductor.

I. INTRODUCTION

The quest for light emitters and sensors operating in the blue or UV regions of the electromagnetic spectrum has tantalized researchers during several decades. Most of the activities in this area concerned the wide band-gap II-VI compounds ZnS and ZnSe with direct band-gap structure and fewer investigations were devoted to the natural challengers of these compounds: the nitrides. Potentialities also exist for the latter in the area of devices operating in hostile conditions.[1] Neither for these II-VI's nor for the nitrides could efficient p doping be realized until very recent years. This issue was resolved when p doping could be achieved in the case of ZnSe via nitrogen substitution of selenide[2] and in GaN by substituting gallium by magnesium.[3] These breakthroughs were immediately followed by the realization of light emitters.[4,5] High-brightness GaN-based light emitting diodes can operate a long time with extremely high ($\sim 10^9$ cm^{-2}) defect densities in contrast with II-VI's where lower densities ($\sim 10^5$–10^6 cm^{-2}) of such crystallographic defects prevent obtainment of a long device operating time.[6] The physics of GaN has long remained in its infancy, but now that materials are available with both high structural and electronic qualities, it is going to rapidly grow up. Nobody knows whether the cubic or hexagonal GaN phase—or both—will be used for large-scale applications, mainly because no lattice-matched substrate exists for realization of pseudomorphic epitaxial growth. As a consequence, sapphire is widely used as a substrate for GaN: It displays a high stability at high temperature and good quality epilayers can be deposited on it in a hexagonal phase. The values of the band gap of this hexagonal phase reported in the literature are scattered.[7–11] This is not understood so far. The purpose of the present paper is to address the physical phenomena responsible for this scattering. We will show that all data are consistent with each other provided that (i) residual strain effects are included in the modeling as well as full contributions of the wurtzite symmetry at the scale of the crystal-field splitting and spin-orbit interaction, and (ii) previous (more than two decades old) work is reexamined for reinterpretation in light of progress made in the knowledge of strain effects in the band structure of semiconductors since these works appeared.

II. OPTICAL PROPERTIES OF GaN EPILAYERS

In a spinless description, the properties of the topmost of the valence band of the "classical" semiconductors can be qualitatively related to the properties of p-like orbitals. In the case of cubic crystal we have a threefold degeneracy which will be lifted by symmetry breaking. Quadrupolar strain fields applied along one highly symmetric orientation like (001) or (111) are efficient symmetry-breaking perturbations giving a valence-band splitting between one single state and a doublet one, when the symmetry of the crystal is lowered from T_d towards D_{2d} or C_{3V}.[12] The wurtzite crystal field also produces a splitting of the triplet state into a doublet and a single state. Microscopically, at the atomic scale the wurtzite lattice differs from the strained zinc-blende lattice when the second neighbors are considered. We anticipate that the correct valence-band symmetries should be derived from the irreducible representations of C_{6V} instead of being obtained from the compatibility tables between T_d and C_{3V} symmetries. Group theory predicts dipole-allowed transitions towards the conduction band, which are submitted to selection rules in σ and π polarization.

The situation becomes more complicated when the valence electron is attributed its spin. In T_d symmetry, a fourfold Γ_8 level is distinguished from a deeper Γ_7 valence-band doublet. The transitions between the conduction band and all these levels are dipole allowed. Any lowering of cubic symmetry of the kinds mentioned above leads to a splitting of the Γ_8 level. When the perturbation is sufficiently symmetric, one state remains uncoupled with the valence band while the second one is coupled by the perturbation with the spin-orbit split-off state. There is a general trend in the III-V and II-VI semiconductors: the splitting of the topmost valence band due to the spin-orbit interaction increases with the atomic number of the anion. This is of crucial importance when nitrogen and oxygen anions are considered in the context of wurtzite symmetry, when both spin-orbit couplings and crystal-field effects are comparable in magnitude. Intricate series of optically active transitions can be observed in an energy range of a few meV, and can only be identified if using selection rules predicted by group theory. Figure 1 displays a reflectivity spectrum taken under $\mathbf{k} \| c$, $\mathbf{E} \perp c$ conditions at 2 K from a 4-μm-thick GaN epilayer deposited in an ASM 12 horizontal MOVPE reactor, at 985 °C, under hydrogen flux, using ammoniac and triethylgallium for precursors,
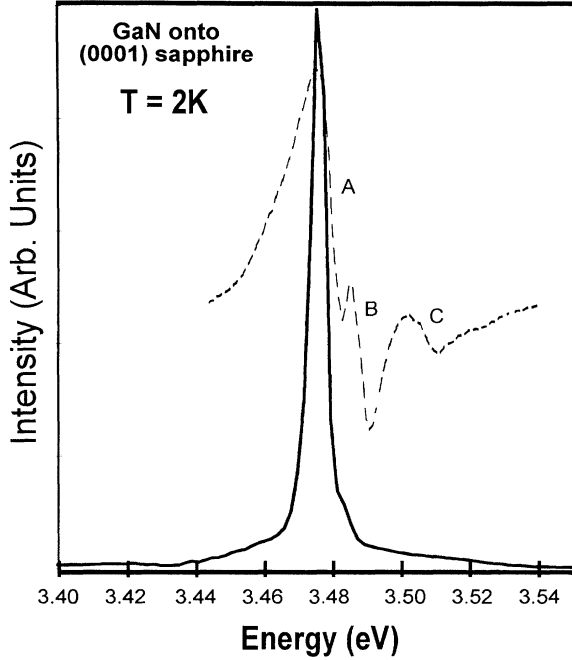
FIG. 1. Typical reflectivity spectrum (dashed line) taken in $k\|c, E\perp c$ conditions at liquid helium temperature on a 4-μm-thick GaN epilayer deposited on sapphire by MOVPE using NH_3 and triethylgallium. The photoluminescence spectrum (full line) is also given for the sake of completeness.

and a sapphire substrate. A GaN buffer layer grown at 550 °C was deposited on sapphire before the epitaxy of the GaN layer begins. This procedure is quite standard and the description of the growth of samples is beyond the scope of this paper; more details will be published elsewhere.[13] The line-shape fitting of the reflectivity spectrum has been made in the context of a dispersive description of dielectric constant[14] using three oscillators and a dead layer thickness of 6 nm. Our finding is consistent with what is called the natural ordering of the valence band, the ordering of wurtzite ZnS, and we easily identify the A, B, and C excitons. Straightforward comparison of our energies with values in the literature evidences serious discrepancy and the scattering of values (see Table I) cannot be attributed to an error in the data analysis, since the optical structures give narrow features. In fact, we have a new set of values. All the samples have different thicknesses, or are grown with various buffer layers intercalated between the sapphire and the epilayer. To evidence correlation between sample structure and peak po-
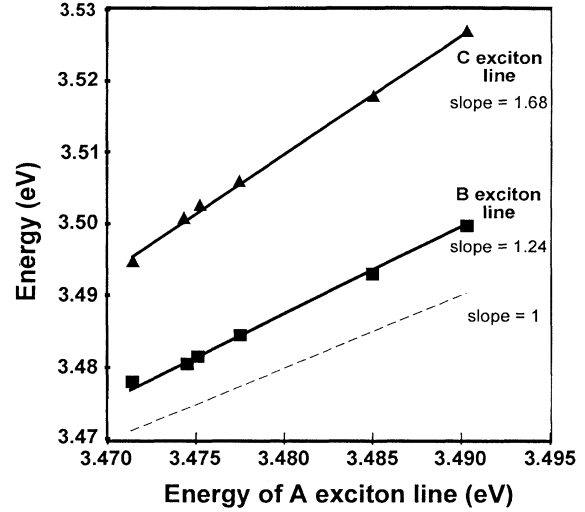

FIG. 2. Plot of the transition energies reported for B and C excitons versus energy position of the A line.

sitions, we suggest to consider all these energies and to plot them as a function of the energy of the fundamental (A) transition. The result of such procedure appears in Fig. 2, where straight lines can be drawn between energies of B and C excitons, and are a nice evidence of the existence of a correlation between these energies. The slopes are 1, 1.24, and 1.68, respectively. One value does not follow the trend, the value of the C exciton published by Monemar.[8] It is clear that misinterpretation of the data occurred in this paper; the 3.503 eV is more likely to be the C exciton rather than the weak 3.4935-eV one. The latter might be attributed to a $2S$ state of the A exciton. This is plausible, since it is fairly weak on the one hand and since this identification leads to a binding energy of 24 meV on the other hand, a value some 4 meV smaller than the value of Dingle and Illegems.[15] At this stage of the paper we have experimental evidence of an influence of residual strain on the transition energies. The next section is devoted to the quantitative interpretation of the data.

III. DATA ANALYSIS

In the most general way the invariant forms, time-reversal symmetric Hamiltonians which describe the influence of a wurtzite field on the conduction and valence band at zone center, write[16]

TABLE I. Low-temperature ($T<10$ K) values reported for the transition energies in a wurtzite GaN epilayer grown on sapphire substrates.

Reference	A line (eV)	B line (eV)	C line (eV)	Thickness (μm)
7 (Fig. 3)	3.4745	3.4805	3.501	150
8	3.4751	3.4815	3.4935/3.503	110
This work	3.4775	3.4845	3.5062	4 + GaN buffer
9	3.485	3.493	3.518	4 + AlN buffer
10	3.4903	3.4997	3.527 05	Not communicated
11	3.471	3.478	3.494	500

$$H_c = E \Xi_{\Gamma 1} \qquad (1)$$

and

$$H_v = \{a + b I_z^2 + c I_z \sigma_z + d(I_x \sigma_x + I_y \sigma_y)\} \Xi_{\Gamma 1}. \qquad (2)$$

Examples of the time-reversal quantity $\Xi_{\Gamma 1}$ which transforms as Γ_1 are the crystal field itself, and for the purpose of the present paper the components of the deformation tensor e_{zz} and $e_{xx} + e_{yy}$. To each $\Xi_{\Gamma 1}$ are associated quantities having a given physical meaning. Consider the wurtzite field itself: a is the average position of the valence bands, b is the crystal-field splitting (Δ_1) in the simple group (see beginning of Sec. II of the paper), and c and d are the two components of the spin-orbit interaction predicted by group theory (respectively, Δ_2 and Δ_3 hereafter). $\Delta_2 = \Delta_3$ in the quasicubic model.[17] We next consider either a hydrostatic pressure or a biaxial compression in the (0001) plane. The nonvanishing components of the strain tensor are e_{zz} and $e_{xx} = e_{yy}$. Two sets of four deformation potentials are to be defined, one set for $\Xi_{\Gamma 1} = e_{zz}$, another set of four for $\Xi_{\Gamma 1} = e_{xx} + e_{yy}$. Now we attribute to a, b, c, and d the following physical meaning: a is the shift of the average valence-band position when the lattice parameter is changed along the (0001) direction. b quantifies the modification of the crystal-field splitting parameter Δ_1, and c and d account for the modifications of the spin-orbit interaction with e_{zz}. These quantities are labeled a_z, b_z, c_z, and d_z, respectively. We define similar quantities a_x, b_x, c_x, and d_x *mutatis mutandis* and we note that modifications of the (already small) spin-orbit interaction are second-order relativistic effects. Thus we neglect them in the light of experimental information available and only keep a_i and b_i deformation potentials. The situation is straightforward for the conduction band where E_i deformation potentials are defined in analogy with a_i. Among the physical quantities accessible via optical spectroscopy are the differences $E_i - a_i$, the analog of the hydrostatic deformation potential in cubic symmetry. Although the analogy is not possible in the strictest sense, we attribute a shear character to the deformation potentials b_i. Using for a basis the eigenvectors for angular momentum $I = 1$ and Pauli matrices for $\sigma = \frac{1}{2}$, and after some elementary manipulations, we get analytical expressions for the stress dependence of the valence-band states, i.e., a linear expression for the Γ_9 state and the classical solutions for a two-level system for the Γ_7 levels (see Appendix). Fitting the whole set of data does not enable us to obtain independently all the deformation potential of the theory described above. Studies of pressure dependence of the near band-gap absorption and of the broad deep photoluminescence band have appeared elsewhere[18–20] for bulk GaN. Although these data do not reveal subtle effects due to modest qualities of the studied samples, they offer important information and some restrictions concerning the values of a_z and a_x. The average pressure coefficient of 4.2 meV/kbar is nothing else than $a_z e_{zz}^h + a_x(e_{xx}^h + e_{yy}^h)$, where here e_{ii}^h are the components of the strain tensor under hydrostatic pressure. This gives a first relation between a_z and a_x. Second, from the ratio of the three slopes at high biaxial stress we obtain

$$\frac{a_z e_{zz}^b + a_x(e_{xx}^b + e_{yy}^b)}{b_z e_{zz}^b + b_x(e_{xx}^b + e_{yy}^b)} = -2.16 \qquad (3)$$

and

$$\frac{\Delta_1 - \Delta_2}{\sqrt{(\Delta_1 - \Delta_2)^2 + 8\Delta_3^2}} \approx 0.44. \qquad (4)$$

There are different strain-inducing processes involved here: the layer has a large lattice mismatch with its substrate; an AlN buffer is sometimes used, which is also mismatched with the substrate and GaN layer; the difference of the thermal expansion coefficient is also generating some stress (compression or dilatation, depending on whether the substrate is sapphire or SiC, respectively). Relaxation will necessarily occur, and a great density of dislocation (10^8–10^{10} cm^{-2}) is always present in these heteroepitaxial layers. As a consequence, it is extremely difficult to speculate on the nature and origin of the stresses at this stage. However, on a sapphire substrate, the compressive strain will lead to an increased band gap. We make the assumption that the lowest transition energies reported in the literature (Monemar *et al.*[11] for a 500-μm layer) correspond to an almost strain-free situation. Using the stiffness coefficients given in Ref. 21, $C_{11} = 296$ GPa, $C_{33} = 267$ GPa, $C_{12} = 130$ GPa, and $C_{13} = 158$ GPa, we obtain the best fit to the data with $\Delta_1 = 10.0 \pm 0.1$ meV, $\Delta_2 = 6.2 \pm 0.1$ meV, and $\Delta_3 = 5.5 \pm 0.1$ meV.

Concerning the deformation potentials, we obtain relations between them. Under hydrostatic pressure we calculate $e_{zz}^h = 1.723\,76 \times 10^{-4}$ kbar^{-1} and $e_{xx}^h = 1.708\,09 \times 10^{-4}$ kbar^{-1}. Using the corresponding data, and making $E_z = E_x = 0$, we obtain $a_z + 2a_x \approx 24.5$ eV. Under biaxial stress $e_{zz}^b = -4.951\,89 \times 10^{-4}$ kbar^{-1} and $e_{xx}^b = 4.184\,03$
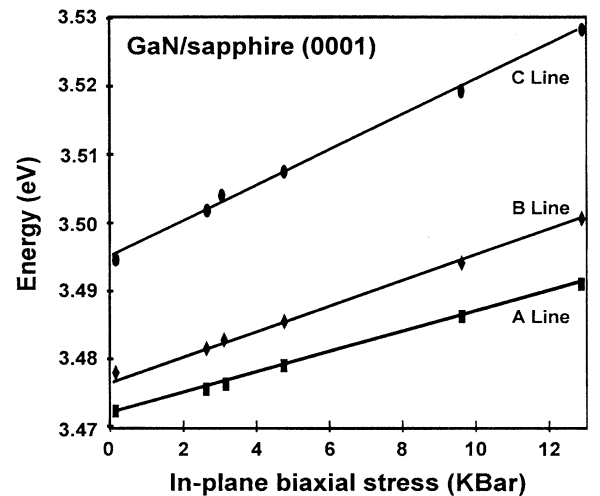

FIG. 3. Dependence of the transition energies of A, B, and C excitons versus in-plane biaxial stress in the epilayer. The experimental data (dots) correspond to the data of Table I. The residual stress is determined by matching the position of the A line with the calculated value.

$\times 10^{-4}$ kbar$^{-1} \approx -0.85 e_{zz}^b$. The fit to the whole set of data gives $a_z + 1.7 a_x \approx -2.16(-b_z + 1.7 b_x)$. If we now wish to compare these results with deformation potentials of some cubic semiconductor, we put $a_x = a_z$, which gives a band-gap deformation potential of -8.16 eV, a value to be compared with the GaAs value.[22] A similar procedure applied for b_z and b_x gives $b = 3.71$ eV. Once again, this value is in the range of values obtained for cubic semiconductors.[22] The data of Fig. 2 have been replotted as a function of the biaxial stress in the epilayer. The result is given in Fig. 3. We note that the agreement with theory is excellent and that GaN epilayers undergo easily more than 10 kbar biaxial compression under the (0001) direction which is not the case for other less robust heteroepitaxial systems like II-VI's on GaAs.

IV. CONCLUSION

The optical properties of GaN hexagonal epilayers deposited on sapphire have been reexamined. We have shown that the scattering of the data in the literature is related to residual strain effects in the layers. The comprehension of the reported results requires us to use two wurtzitelike parameters to account for the spin-orbit interaction in the valence band. Relationships are obtained which connect the four principal deformation potentials together in wurtzite GaN.

ACKNOWLEDGMENT

APPENDIX

We choose for representations basis sets such that operators I_z and σ_z are given by the following matrices:

$$\begin{pmatrix} 1 & 0 & 0 \\ 0 & 0 & 0 \\ 0 & 0 & -1 \end{pmatrix} \quad \text{and} \quad \begin{pmatrix} 1 & 0 \\ 0 & -1 \end{pmatrix},$$

respectively. Projecting Eq. (2) we obtain

$$E(\Gamma_{9V}) = E_0 + \Delta_1 + \Delta_2 a_z e_{zz} + a_x(e_{xx} + e_{yy}) + b_z e_{zz} + b_x(e_{xx} + e_{yy}),$$

$$E(\Gamma_{7V}^{\pm}) = E_0 + \frac{\Delta_1 - \Delta_2}{2} + a_z e_{zz} + a_x(e_{xx} + e_{yy}) + \frac{b_z e_{zz} + b_x(e_{xx} + e_{yy})}{2} \pm \frac{\sqrt{[\Delta_1 - \Delta_2 + b_z e_{zz} + b_x(e_{xx} + e_{yy})]^2 + 8\Delta_3^2}}{2}.$$

In the range of linear dependence with stress, introducing the zero stress values $E^0(\Gamma_{7V}^{\pm})$ we obtain expressions[23]

$$E(\Gamma_{7V}^{\pm}) = E^0(\Gamma_{7V}^{\pm}) + a_z e_{zz} + a_x(e_{xx} + e_{yy}) + \frac{b_z e_{zz} + b_x(e_{xx} + e_{yy})}{2}\left(1 \pm \frac{\Delta_1 - \Delta_2}{\sqrt{(\Delta_1 - \Delta_2)^2 + 8\Delta_3^2}}\right).$$

[1] H. Morkoç, S. Strite, G. B. Gao, M. E. Lin, B. Sversdlov, and M. Burns, J. Appl. Phys. **73**, 1363 (1994).

[2] R. M. Park, M. B. Troffer, C. M. Rouleau, J. M. Depuydt, and M. A. Haase, Appl. Phys. Lett. **57**, 2127 (1990).

[3] H. Amano, M. Kito, K. Hiramatsu, and I. Akasaki, Jpn. J. Appl. Phys. **28**, L2112 (1989).

[4] M. A. Haase, J. Qiu, J. M. Depuydt, and H. Cheng, Appl. Phys. Lett. **59**, 1972 (1991).

[5] S. Nakamura, T. Mukai, and M. Senoh, Appl. Phys. Lett. **64**, 1687 (1994).

[6] K. Shazad, J. Petruzello, D. J. Olego, D. A. Cammack, and J. M. Gaines, Appl. Phys. Lett, **57**, 2452 (1990); G. C. Hua, N. Otsuka, D. C. Grillo, Y. Fan, J. Han, M. D. Ringle, R. L. Gunshor, M. Hovinen, and A. V. Nurmikko, Appl. Phys. Lett. **65**, 1331 (1995).

[7] R. Dingle, D. D. Sell, S. E. Stokowski, and M. Illegems, Phys. Rev. B **4**, 1211 (1971).

[8] B. Monemar, Phys. Rev. B **10**, 676 (1974).

[9] W. Shan, T. J. Schmidt, X. H. Yang, S. J. Hwang, and J. J. Song, Appl. Phys. Lett. **66**, 987 (1995).

[10] H. Morkoç (private communication); (unpublished).

[11] B. Monemar, P. Bergman, H. Amano, and I. Akasaki (unpublished).

[12] We use the notations of Koster, Dimmock, Wheeler, and Statz, in *Properties of the Thirty-Two Point Groups* (MIT Press, Cambridge, 1963).

[13] O. Briot, B. Gil, S. Sanchez, and R. L. Aulombard (unpublished).

[14] S. J. Pekar, Zh Éksp. Teor. Fiz. **33**, 1022 (1957) [Sov. Phys. JETP. **6**, 785 (1958)]; **33**, 1056 (1957) [**6**, 813 (1958)]; Fiz. Tverd. Tela **4**, 1301 (1962) [Sov. Phys. Solid State **4**, 953 (1962)].

[15] R. Dingle and M. Illegems, Solid State Commun. **9**, 175 (1971).

[16] K. Cho, Phys. Rev. B **14**, 4463 (1976).

[17] J. J. Hopfield, J. Phys. Chem. Solids **15**, 97 (1960).

[18] D. L. Camphausen, G. A. Neville Connel, and W. Paul, Phys. Rev. Lett. **26**, 184 (1971).

[19] P. Perlin, I. Gorczyca, N. E. Christensen, I. Grzegory, H. Teisseyre, and T. Suski, Phys. Rev. B **45**, 13 307 (1992).

[20] H. Teisseyre, P. Perlin, T. Suski, I. Grzegory, J. Jun, and S. Porowski, J. Phys. Chem. Solids **56**, 353 (1995).

[21] *Semiconductors: Group IV Elements and III-V Compounds*, edited by O. Madelung (Springer-Verlag, Berlin, 1991).

[22] A. Gavini and M. Cardona, Phys. Rev. B **1**, 672 (1970).

[23] V. B. Sandomirskii, Fiz. Tverd. Tela **6**, 324 (1964) [Sov. Phys. Solids State **6**, 261 (1964)].